Molecular Modeling Connect
ISSN: 3105-3734
2026, Article ID. 2026.0020, Cite as: https://doi.org/10.69709/MolModC.2026.199313

SCIFINITI PUBLISHING

Research Article

OPEN ACCESS

Molecular Docking and ADME Profiling of *N*-(Substituted-1,3-benzothiazol-2-yl)benzamide Derivatives as Potential Anticonvulsant Agents

Ahmed Rufa'i[✉,1,*], **Abdullahi Y. Idris**[✉,2], **Aliyu M. Musa**[✉,2], **Halimatu S. Hassan**[✉,2], **Asma'u H. Nasiru**[✉,2], **Mohammed G. Magaji**[✉,3], **Rabiu Bako**[✉,4], **Muhammad Sa'idu**[✉,5], **Isah J. Muhammad**[✉,6]

[1] Department of Pharmaceutical and Medicinal Chemistry, Faculty of Pharmaceutical Sciences, Gombe State University, Gombe 760101, Nigeria
[2] Department of Pharmaceutical and Medicinal Chemistry, Faculty of Pharmaceutical Sciences, Ahmadu Bello University, Zaria, Nigeria
[3] Department of Pharmacology and Therapeutics, Faculty of Pharmaceutical Sciences, Ahmadu Bello University, Zaria, Nigeria
[4] Department of Pharmaceutical and Medicinal Chemistry, Faculty of Pharmaceutical Sciences, Kaduna State University, Kaduna, Nigeria
[5] Department of Pure and Applied Chemistry, Faculty of Physical Sciences, Kaduna State University, Kaduna, Nigeria
[6] Department of Pharmaceutical and Medicinal Chemistry, Faculty of Pharmaceutical Sciences, Ibrahim Badamasi Babangida University, Lapai, Niger 920001, Nigeria

Article History
Received: December 01, 2025 Accepted: July 25, 2026 Published: August 25, 2026

Abstract
Amides represent a class of organic compounds with diverse biological activity and notable anticonvulsant properties. This study aimed to evaluate the pharmacokinetic properties and molecular interactions of 15 N-(substituted-1,3-benzothiazol-2-yl)benzamide derivatives against two key epilepsy-related targets, γ-aminobutyric acid aminotransferase (GABA-AT) and the activated open sodium ion channel, in order to assess their potential anticonvulsant activity. Crystal structures of GABA-AT (PDB ID: 1OHW) and the sodium ion channel (PDB ID: 5HVX) were obtained from the RCSB Protein Data Bank, and molecular docking was performed using AutoDock Vina following protein preparation in Chimera v1.11.2. Post-docking analysis was conducted using Chimera and Discovery Studio Visualizer, and ADME properties were also predicted. ADME analysis showed high gastrointestinal absorption for all compounds except compound 5. Docking results revealed that seven compounds (Cp1, Cp3, Cp7, Cp10, Cp12, Cp13, and Cp14) exhibited interaction profiles similar to vigabatrin, while three (Cp10, Cp13, and Cp14) showed interaction profiles similar to those of lamotrigine, and all demonstrated favorable binding interactions with both targets. Overall, the docking analysis identified selected N-(substituted-1,3-benzothiazol-2-yl)benzamide derivatives—particularly Cp1, Cp3, Cp7, Cp10, Cp12, Cp13, and Cp14—as the most promising lead candidates, with significant potential for anticonvulsant activity.

Keywords:
activated open sodium ion channel; amides; Absorption Distribution Metabolism and Elimination; epilepsy; Gamma-Aminobutyric Acid-Aminotransferase; *in silico* studies

1. Introduction

Epilepsy is one of the most prevalent chronic neurological disorders, affecting approximately 50 million people worldwide and contributing significantly to premature mortality, particularly in low- and middle-income countries where access to treatment remains limited [1]. Despite advances in antiepileptic drug development, many currently available therapies carry significant limitations, including dose-related toxicity, idiosyncratic adverse effects, and poor long-term efficacy; common side effects

* **Corresponding Author:**
Ahmed Rufa'i, Department of Pharmaceutical and Medicinal Chemistry, Faculty of Pharmaceutical Sciences, Gombe State University, Gombe 760101, Nigeria, roofmoon4cool@gmail.com

© 2026 Copyright by the Authors.
Licensed as an open access article using a CC BY 4.0 license.

such as hepatotoxicity, ataxia, and hematological abnormalities continue to compromise patient compliance and therapeutic outcomes [2,3]. Despite the development of newer anticonvulsants, first-generation drugs such as phenobarbital, phenytoin, carbamazepine, valproic acid, zonisamide, and clobazam remain widely used despite these significant limitations.

Newer agents, such as lamotrigine, topiramate, tiagabine, pregabalin, and stiripentol, are similarly linked to toxicity and limited long-term efficacy [4,5]. Furthermore, a significant proportion of patients have drug-resistant epilepsy, underscoring the urgent need for safer and more effective therapeutic agents; despite the rapid development of antiepileptic drugs, rational optimization of anticonvulsant design therefore remains crucial [6,7]. Identifying new scaffolds with improved pharmacological properties has been a central focus of recent medicinal chemistry efforts. Amides are one class of compounds that have shown significant anticonvulsant potential [8–10], with structural characteristics such as hydrogen bonding capacity and hydrophobic interactions that make them attractive candidates for drug design. Benzothiazole derivatives are likewise recognized as adaptable pharmacophores with a range of biological activities, including antitubercular, antibacterial, anticonvulsant, antidiabetic, anticancer, anthelmintic, analgesic, anti-inflammatory, and antitumor properties [11,12].

γ-aminobutyric acid (GABA) and voltage-gated sodium channels (Navs) are essential for controlling neuronal excitability in the central nervous system: while elevated GABA levels help suppress seizures, decreased GABA levels can trigger convulsions [13]. The first inward current during action potential depolarization arises from voltage-gated sodium channels, which are linked to increased excitatory (glutamatergic) activity and decreased inhibitory (GABAergic) transmission, both of which contribute to seizure development [14,15]. Molecular docking, which uses search algorithms and scoring systems to predict optimal ligand binding, is a reliable computational method for studying drug-target interactions; these *in silico* techniques advance drug development by providing insight into pharmacokinetic characteristics, binding affinity, and interaction mechanisms [16–18]. Because the etiology of epilepsy involves both impaired GABAergic inhibition and abnormal sodium channel activity, a dual-target strategy may offer greater therapeutic benefit. To identify promising candidates with enhanced anticonvulsant potential, this study therefore uses molecular docking and *in silico* ADME analysis to examine the interaction profiles and pharmacokinetic characteristics of N-(substituted-1,3-benzothiazol-2-yl)benzamide derivatives against GABA-AT and the activated open sodium channel. These two well-established therapeutic targets—GABA-AT and the voltage-gated sodium channel model Nav*Ms*—were selected for their critical roles in enhancing inhibitory neurotransmission and suppressing neuronal hyperexcitability.

2. Materials and Methods

2.1. Computational Tools

The study utilized the following computational tools: MarvinSketch (v20.20), Spartan '14 (v1.1.4), AutoDockTools (v1.5.6), UCSF Chimera (v1.11.2), Discovery Studio Visualizer (v20.1.0.19295), and the SwissADME online platform.

2.2. Docking Analysis

Molecular docking was employed as a robust computational method to elucidate the intermolecular interactions between the newly designed compounds and their target receptors, and to provide preliminary estimates of their binding affinities.

2.3. Ligand Preparation

The MarvinSketch (v20.20) program was used to generate all chemical structures, which were saved as an MDL SD file and then incorporated into Spartan software (Spartan 14). All structures were subsequently optimized using the molecular mechanics force field (MMFF) and saved in Sybyl Mol2 format. Ligands were prepared following standard protocols, including structural energy minimization, hydrogen addition, and Gasteiger charge computation, as previously described [19].

2.4. Protein Preparation

The protein targets—GABA aminotransferase (GABA-AT; PDB ID: 1OHW) and Nav*Ms* (PDB ID: 5HVX)—were obtained from the RCSB Protein Data Bank and prepared using UCSF Chimera (v1.11.2) and AutoDockTools (v1.5.6), following the standard protein preparation protocol, which included removal of all water molecules from the complex structures. During a brief relaxation step, hydrogen atoms and charges were added, and the crystal structures were minimized with optimization of the hydrogen-bonding network. Ligands were prepared through a separate ligand preparation procedure involving energy minimization, hydrogen addition, and Gasteiger charge assignment. Docking used the cavity detection algorithm, with 10 runs, a population size of 150, a crossover rate of 0.8, and 27,000 maximum generations [19].

2026, Vol. 3, Article ID. 2026.0020
https://doi.org/10.69709/MolModC.2026.199313

2.5. Molecular Docking Evaluation

Molecular docking was conducted with the receptor held in a rigid conformation, while the ligand was permitted to adopt a flexible conformation. Docking was carried out using AutoDock Vina, the virtual-screening software developed by Trott and Olson [20]. Table 1 presents the grid box parameters used for each enzyme.

Table 1: Grid-box dimensions for each enzyme.

Enzyme	PDB	Grid Box Size			Center		
		X	Y	Z	X	Y	Z
GABA-AT	1OHW	20	28	18	11.228	−0.47	18.337
Nav*Ms*	5HVX	42	46	38	65.379	62.014	17.982

X, Y, Z represent 3D geometric axes.

2.6. Docking Validation

The docking process was validated prior to screening the test compounds by first removing the co-crystallized ligand from the enzyme structure obtained from the Protein Data Bank, then re-docking it using the same docking parameters, yielding root-mean-square deviation (RMSD) values of 0.9632 Å and 1.02 Å for GABA-AT and Nav*Ms*, respectively. Successful validation was confirmed when the re-docked pose closely superimposed on the original geometric conformation of the co-crystallized ligand within the active site, as assessed using the virtual screening software (AutoDock Vina), with the resulting poses visualized in Discovery Studio 2020 Client [21].

2.7. Post-Docking Analysis

Grid box dimensions were established based on the native ligand, and post-docking analyses were carried out using Chimera and Discovery Studio Visualizer to evaluate ligand-enzyme interactions. The leading docking poses were identified, and the conformation exhibiting the essential binding interactions was selected for further analysis.

2.8. Evaluation of Pharmacokinetic and ADME Properties

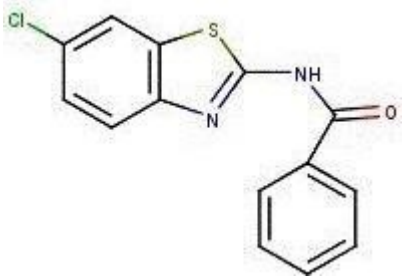
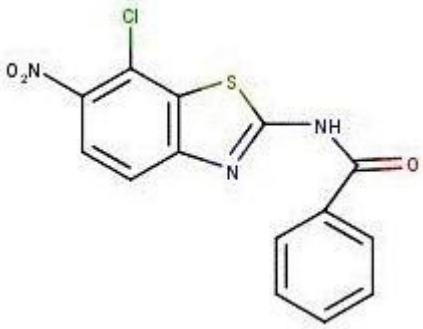
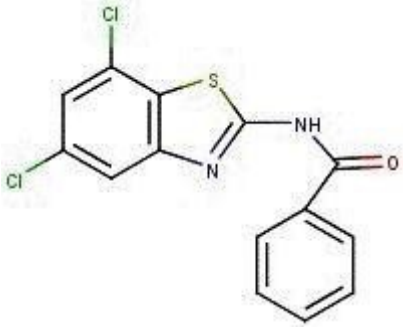
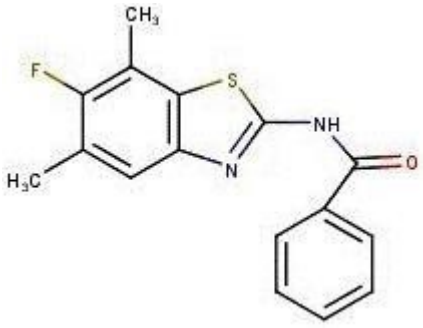
Before proceeding to cell-based and animal experiments, SwissADME—a comprehensive predictive ADME platform—was used to predict the pharmacokinetic and ADME features of the selected hit and lead compounds. Unfavorable pharmacokinetic (PK) properties have historically been a leading cause of compound failure in later stages of drug development [22], often stemming from a failure to recognize and address poor pharmacokinetic features in lead series approved for further optimization. As high-throughput screening, combinatorial chemistry, and parallel synthesis have become integral to drug discovery, early characterization of a compound's absorption, distribution, metabolism, and elimination (ADME) has become essential to lead selection and optimization [23,24]. Notably, Lipinski et al. [25] conducted a landmark study examining orally active compounds to identify the physicochemical ranges associated with a high likelihood of oral bioavailability [26–28].

3. Results and Discussion

3.1. Molecular Docking

GABA-AT represents a promising target for antiepileptic therapy, since selective inhibition of this enzyme raises GABA concentrations in the brain. Vigabatrin (γ-vinyl-GABA), an established antiepileptic drug, has been widely studied using various biochemical techniques, generating multiple hypotheses regarding its enzyme-inactivating mechanisms and the resulting elevation of γ-aminobutyric acid levels in central neurons. For each compound, the docking pose with the highest score was selected based on its interaction energy with GABA-AT [29]. Compounds Cp1, Cp3, Cp7, Cp10, Cp12, Cp13, and Cp14 showed substantial binding affinities toward GABA-AT, comparable to the reference inhibitor vigabatrin, according to the docking scores listed in Table 2. A thorough review of the literature further identified the key amino acid residues within the GABA-AT active site [10,30,31].

Table 2: Molecular structures accompanied by the compounds' bioaffinity scores.

S/N	Molecular Structure	Bioaffinity (kcal/mol) for 1OHW	Bioaffinity (kcal/mol) for 5HVX
Compound 1	 N-(6-chloro-1,3-benzothiazol-2-yl)benzamide (Cp1)	**−6.5**	**−5.6**
Compound 2	 N-(7-chloro-6-nitro-1,3-benzothiazol-2-yl)benzamide (Cp2)	**−6.7**	**−5.2**
Compound 3	 N-(5,7-dichloro-1,3-benzothiazol-2-yl)benzamide (Cp3)	**−7.3**	**−5.5**
Compound 4	 N-(6-fluoro-5,7-dimethyl-1,3-benzothiazol-2-yl)benzamide (Cp4)	**−7.4**	**−6.4**

2026, Vol. 3, Article ID. 2026.0020
https://doi.org/10.69709/MolModC.2026.199313

Table 2: *Cont.*

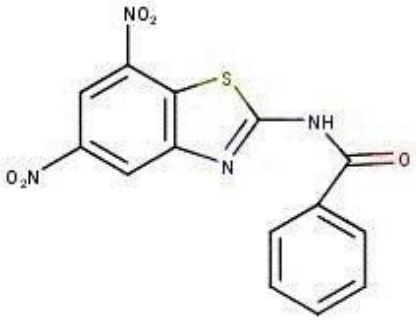
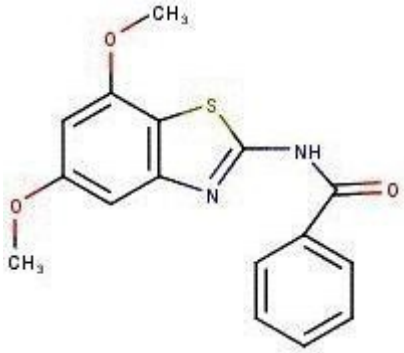
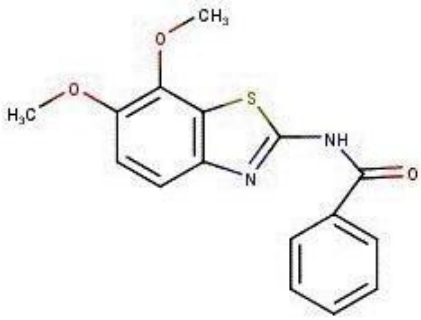
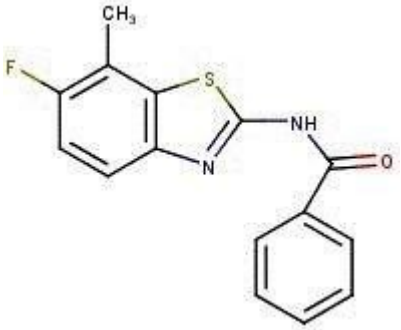
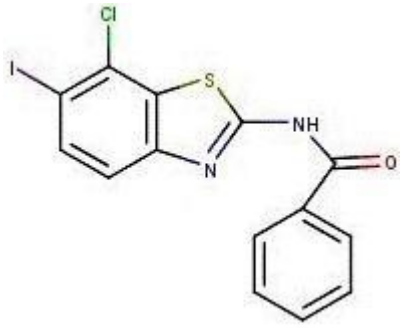
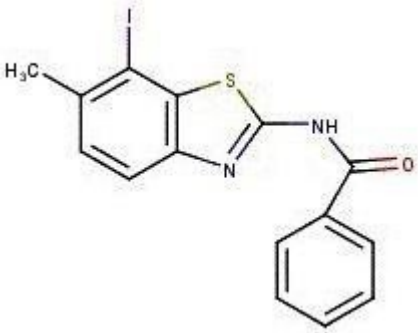
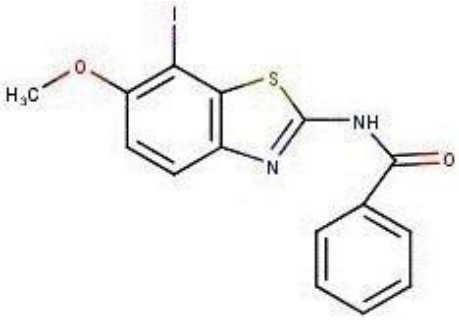
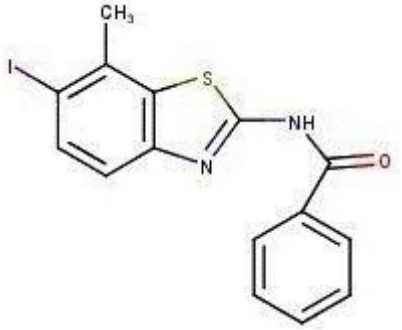
S/N	Molecular Structure	Bioaffinity (kcal/mol) for 1OHW	Bioaffinity (kcal/mol) for 5HVX
Compound 5	 N-(5,7-dinitro-1,3-benzothiazol-2-yl)benzamide (Cp5)	**−7.3**	**−5.6**
Compound 6	 N-(5,7-dimethoxy-1,3-benzothiazol-2-yl)benzamide (Cp6)	**−7.0**	**−4.6**
Compound 7	 N-(6,7-dimethoxy-1,3-benzothiazol-2-yl)benzamide (Cp7)	**−7.6**	**−4.9**
Compound 8	 N-(6-fluoro-7-methyl-1,3-benzothiazol-2-yl)benzamide (Cp8)	**−7.1**	**−6.2**

Table 2: *Cont.*

S/N	Molecular Structure	Bioaffinity (kcal/mol) for 1OHW	Bioaffinity (kcal/mol) for 5HVX
Compound 9	 N-(7-chloro-6-iodo-1,3-benzothiazol-2-yl)benzamide (Cp9)	**−6.9**	**−6.2**
Compound 10	 N-(7-iodo-6-methyl-1,3-benzothiazol-2-yl)benzamide (Cp10)	**−7.7**	**−6.3**
Compound 11	 N-(7-iodo-6-methoxy-1,3-benzothiazol-2-yl)benzamide (Cp11)	**−7.5**	**−4.8**
Compound 12	 N-(6-iodo-7-methyl-1,3-benzothiazol-2-yl)benzamide (Cp12)	**−6.4**	**−5.5**

2026, Vol. 3, Article ID. 2026.0020
https://doi.org/10.69709/MolModC.2026.199313

Table 2: *Cont.*

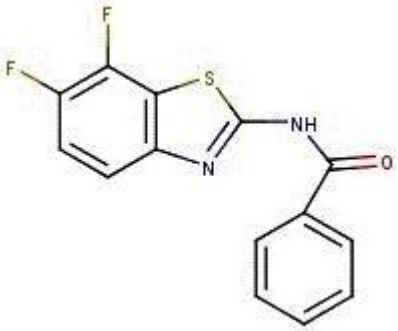
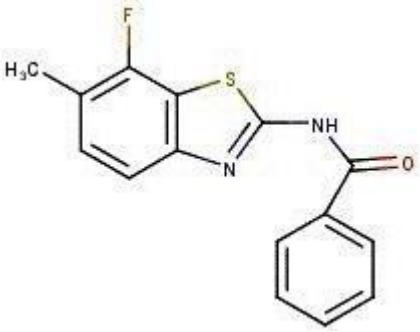
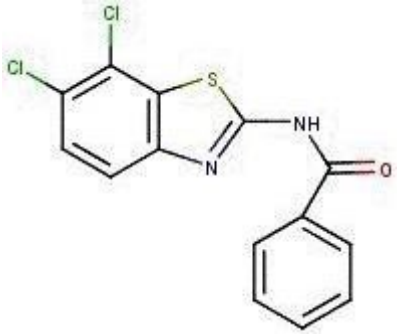
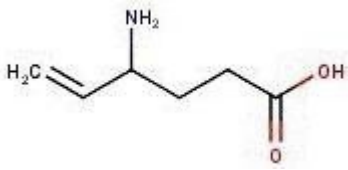
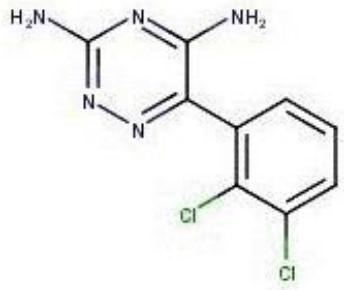
S/N	Molecular Structure	Bioaffinity (kcal/mol) for 1OHW	Bioaffinity (kcal/mol) for 5HVX
Compound 13	 N-(6,7-difluoro-1,3-benzothiazol-2-yl)benzamide (Cp13)	**−6.6**	**−5.4**
Compound 14	 N-(7-fluoro-6-methyl-1,3-benzothiazol-2-yl)benzamide (Cp14)	**−7.4**	**−5.4**
Compound 15	 N-(6,7-dichloro-1,3-benzothiazol-2-yl)benzamide (Cp15)	**−7.0**	**−6.6**
Reference (Vigabatrin)		**−5.2**	–

Table 2: *Cont.*

S/N	Molecular Structure	Bioaffinity (kcal/mol) for 1OHW	Bioaffinity (kcal/mol) for 5HVX
Reference (Lamotrigine)		—	**−5.0**

Note: 1OHW corresponds to γ-aminobutyric acid aminotransferase (GABA-AT), and 5HVX represents the activated sodium channel.

Figure 1 shows the bioaffinity values of the top-ranked compounds docked against γ-aminobutyric acid aminotransferase (GABA-AT) and *NavMs*, highlighting their respective binding interaction potentials toward both molecular targets. In molecular docking studies, more negative bioaffinity (binding-energy) values typically indicate stronger ligand-receptor interactions and greater anticipated binding stability.

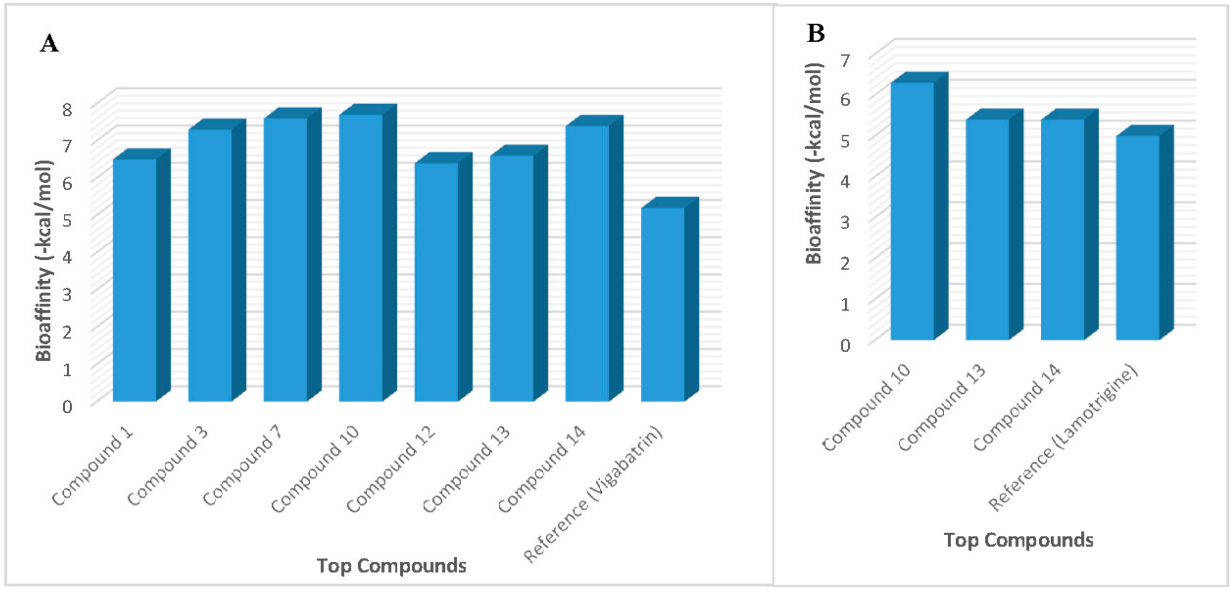


Figure 1: Binding affinity values of the top-ranked compounds toward (**A**) GABA-AT and (**B**) Nav*Ms*.

The docking protocol's validity was confirmed by re-docking vigabatrin into the active site and accurately reproducing its binding orientation and interaction profile, as shown in Figures 2 and 3. The vigabatrin carbonyl group interacts with Ser137 and Gly191 through conventional hydrogen bonding and carbon-hydrogen bonding, while the NH group forms salt bridges with Asp298 and conventional hydrogen bonds with Phe189. Alkyl interactions with Val300 and van der Waals contacts with Gly136, Asp140, His190, Arg192, Ser269, Gln301, and Lys329 provide additional stability (Figure 3).

2026, Vol. 3, Article ID. 2026.0020
https://doi.org/10.69709/MolModC.2026.199313

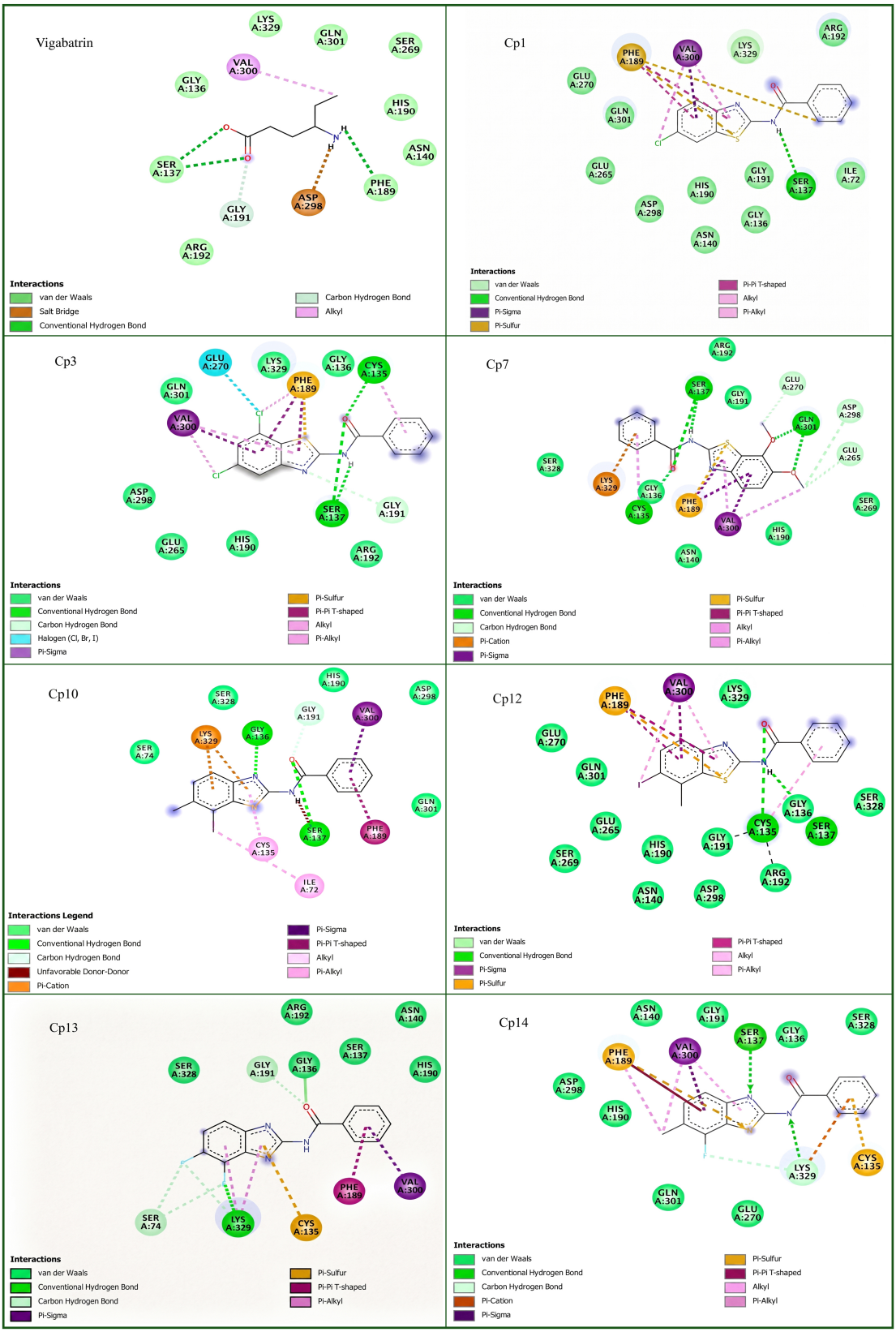


Figure 2: Comparison of molecular surface and 2D interaction patterns of vigabatrin and selected compounds (Cp1, Cp3, Cp7, Cp10, Cp12, Cp13, and Cp14) within the GABA-AT active site.

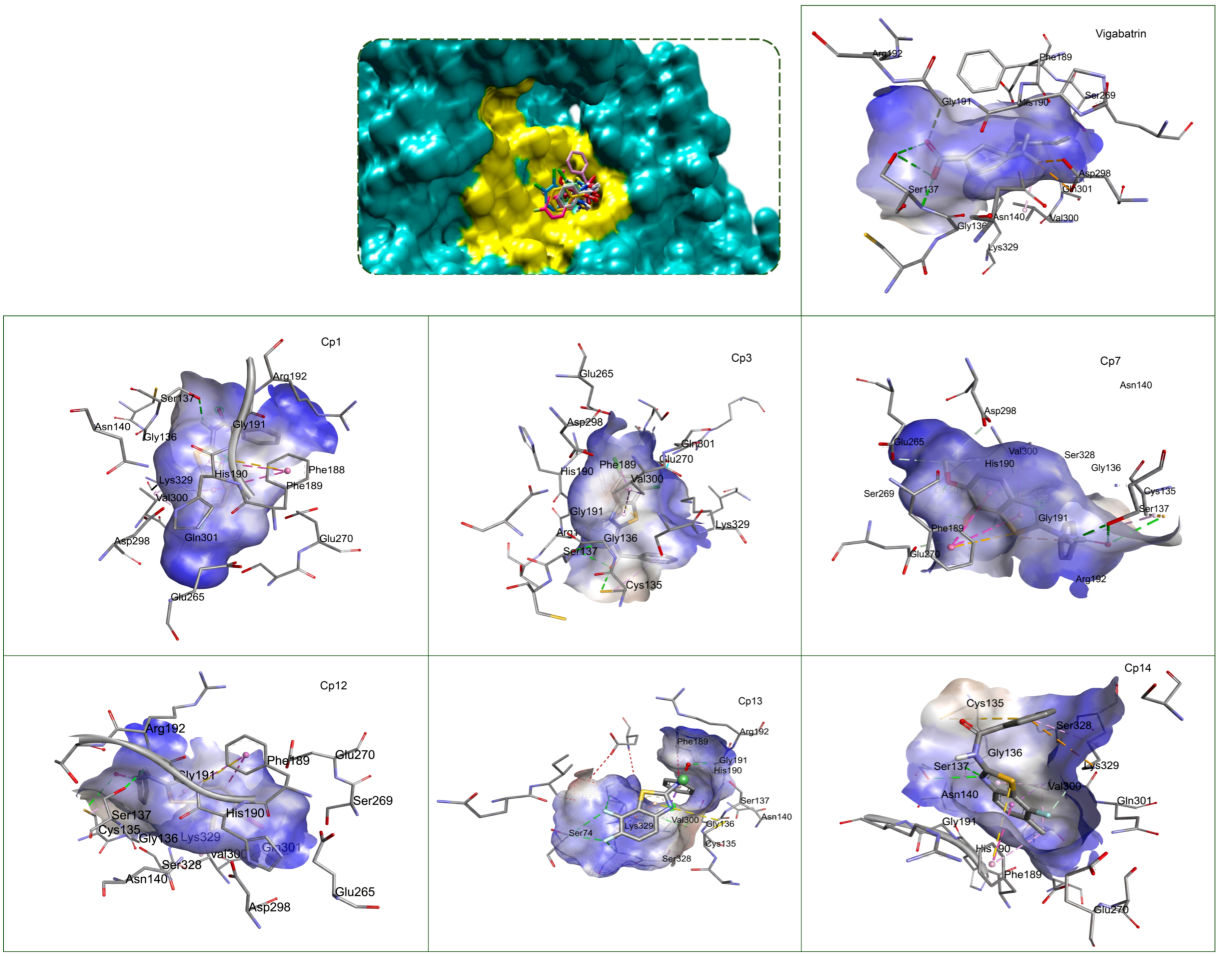


Figure 3: Structural depiction of 3D interactions between vigabatrin and selected compounds (Cp1, Cp3, Cp7, Cp12, Cp13, and Cp14) at the GABA-AT active site.

Table 3 compares these findings with the re-docked vigabatrin pose and its location within the GABA-AT PDB structure. Notably, the best-performing compounds—Cp1, Cp3, Cp7, Cp10, Cp12, Cp13, and Cp14—retained these key contacts, particularly van der Waals interactions with residues such as Gly136, His190, Arg192, Gln301, and Lys329, and conventional hydrogen bonding with Ser137, suggesting that the proposed compounds adopt binding conformations within the catalytic pocket similar to vigabatrin. Several additional stabilizing contacts were also observed, including conventional hydrogen bonding with Gln301 and Gly136 and π-cation interactions of Cp7 and Cp10 with Lys329; consistent with recent studies emphasizing the importance of multipoint interactions in enhancing ligand-enzyme stability and inhibitory activity, these additional contacts may further improve binding affinity and specificity. Together with the visual overlap of ligand poses seen in the docking images, these findings confirm that the compounds successfully occupy the GABA-AT active site, supporting their potential as competitive or mechanism-based inhibitors.

As shown in Table 4, docking studies focused on the Nav*Ms* channel shed light on the compounds' capacity to modulate sodium channel function, a mechanism crucial for seizure regulation. Although Nav*Ms* remains limited as a structurally resolved surrogate model—owing to its prokaryotic homotetrameric architecture, the absence of auxiliary β-subunits, and differences in pore-lining residues relative to mammalian voltage-gated sodium channels—the Nav*Ms* structure used here is, to date, the only sodium channel crystal structure in which all domains are fully resolved. Notably, it features an activated voltage sensor and a pore gate wide enough to permit sodium ion permeation, consistent with an open-channel conformation, making it well suited for molecular dynamics simulations of ion translocation.

2026, Vol. 3, Article ID. 2026.0020
https://doi.org/10.69709/MolModC.2026.199313

Table 3: Docking-based comparison of the binding interactions of vigabatrin (reference drug) and fifteen N-(substituted-1,3-benzothiazol-2-yl)benzamide derivatives with GABA-AT.

Ligand/Compound	Amino Acid Residues Forming Hydrogen Bonds with the Ligand	Active-Site Residues Involved in Ligand Interactions
1	SER137	ILE72, GLY136, ASN140, HIS190, GLY191, ARG192, SER269, GLU270, ASP298, GLN301, LYS329, PHE189, VAL300
2	SER74, SER137, GLY191	GLN71, GLY136, GLU270, GLN301, SER328, PHE189, CYS135, VAL300, LYS329
3	CYS135, SER137, GLY191	CYS135, GLY136, PHE189, HIS190, ARG192, GLU265, GLU270, ASP298, VAL300, GLN301, LYS329
4	HIS190	ILE72, GLY136, ASN140, PHE189, GLY191, ARG192, GLU265, SER269, GLU270, VAL300, GLN301, LYS329
5	SER137, ASN140, GLN301, GLY191, SER269	ILE72, CYS135, GLY136, PHE189, HIS190, ARG192, GLU265, GLU270, ASP298, VAL300, LYS329
6	CYS135, SER137, GLN301, GLU270	GLY136, ASN140, PHE189, HIS190, GLY191, ARG192, GLU265, ASP298, VAL300, SER328
7	CYS135, SER137, GLN301, GLU265, GLU270, ASP298	CYS135, GLY136, ASN140, PHE189, HIS190, GLY191, ARG192, SER269, VAL300, SER328, LYS329
8	ASN140, GLU270, GLN301,	ILE72, GLY136, SER137, PHE189, HIS190, GLY191, ARG192, ASP298, VAL300, LYS329, ARG445,
9	SER137, GLY191	GLN71, ILE72, SER74, CYS135, GLY136, ASN140, PHE189, HIS190, ASP298, VAL300, GLN301, SER328, LYS329
10	GLY136, SER137, GLY191	ILE72, SER74, CYS135, SER137, PHE189, HIS190, ASP298, VAL300, GLN301, SER328, LYS329
11	SER137, GLN301, ASP298	CYS135, GLY136, ASN140, PHE189, HIS190, GLY191, GLU265, GLU270, VAL300, SER328, LYS329
12	CYS135, SER137	CYS135, GLY136, ASN140, PHE189, HIS190, GLY191, ARG192, GLU265, SER269, GLU270, ASP298, VAL300, GLN301, SER328, LYS329
13	SER74, GLY191, LYS329	CYS135, GLY136, SER137, ASN140, PHE189, HIS190, ARG192, VAL300, SER328, LYS329
14	SER137, LYS329	CYS135, GLY136, ASN140, PHE189, HIS190, GLY191, GLU270, ASP298, VAL300, GLN301, SER328, LYS329
15	GLY136, SER137, GLY191	GLN71, ILE72, SER74, CYS135, SER137, ASN140, PHE189, HIS190, ASP298, VAL300, GLN301, SER328, LYS329
Reference (Vigabatrin)	SER137, PHE189, GLY191	GLY136, ASN140, HIS190, ARG192, SER269, GLN301, LYS329, VAL300, ASP298

The structure further reveals previously uncharacterized interdomain interactions, offering a structural framework for understanding the coupling between voltage-sensor activation and pore-gate opening. Overall, *the* Nav*Ms* structure delivers key mechanistic insights into sodium channel function, including: (i) the physical linkage between voltage-sensor activation and pore-gate opening; (ii) the important role of the C-terminal domain in stabilizing the open-channel conformation and regulating gating dynamics; (iii) a conserved interaction motif shared by prokaryotic and eukaryotic sodium channels; and (iv) structural features that distinguish sodium channels from other ion channel families. These findings suggest that the Nav*Ms* channel may serve as a suitable model for characterizing and identifying blockers of eukaryotic sodium channels [32].

Table 4: Docking-based comparison of the binding interactions of lamotrigine (reference drug) and fifteen N-(substituted-1,3-benzothiazol-2-yl)benzamide derivatives with the activated open sodium ion channel.

Ligand/Compound	Amino Acid Residues Forming Hydrogen Bonds with the Ligand	Active-Site Residues Involved in Ligand Interactions
1	GLY76	TRP77, PHE80,LEU125, LEU126, LEU128
2	LEU177, SER179, TRP180	SER181, TRP180, ILE200, ILE203, LEU125
3	TYR153, ALA195	MET148, HIS192, ASN194, PHE198, LEU152, VAL197, TYR153
4	THR139	LEU138, PHE142, LEU168, PHE172, TYR169
5	TRP77	LYS63, PHE80, VAL121, GLN122, LEU125, LEU126, THR139
6	-	GLY76, VAL121, GLN122, TRP77, PHE80, MET108, LEU125, LEU126
7	TYR153, TRP180, PHE198	MET148, LEU152, PRO193, ASN194, HIS192, ALA195, VAL197
8	GLY76	TRP77, LEU79, VAL83, PHE80, VAL121, LEU125, ALA195, VAL197
9	THR139	LEU138, PHE142, TYR143, LEU168, PHE172, TYR169
10	-	ILE144, LEU152, VAL197, PRO201, PHE202, LEU205, PHE80, VAL141, ALA145, THR139
11	-	PHE157, PRO158, GLU159, PRO187, ASN190, TRP160
12	MET175	LEU177, THR207, PHE214, PHE172, VAL210, LEU211
13	MET175	LEU177, THR207, PHE172, PHE214, VAL210, LEU211, THR176
14	TYR153, PHE189	MET148, LEU152, HIS192, PRO193, ASN194, ALA195, VAL197
15	TRP77	GLU10, GLN15, LYS63, SER75, ASN78, SER112, VAL113, ARG119, GLN122, ARG118
Reference (Lamotrigine)	VAL141, PHE198	ALA145, MET148, ILE174, VAL197, PHE198, PRO201, PHE202, LEU205

Electrophysiological studies of Nav*Ms* channels containing mutations in surrounding residues have validated the proposed binding site, and literature reports have similarly identified key amino acid residues involved in the Nav*Ms* binding site [33–35].

Re-docking of the reference drug lamotrigine (Figures 4 and 5) reproduced its characteristic interactions, including conventional hydrogen bonding with Val141 and Phe198, π–π stacking with Phe198, and hydrophobic interactions involving residues such as Ile144, Met148, and Phe202—results consistent with electrophysiological and crystallographic studies identifying the canonical sodium channel binding pocket. Among the derivatives tested, Cp10, Cp13, and Cp14 showed binding modes similar to lamotrigine, occupying the same binding site and displaying comparable interaction profiles; these compounds formed important hydrophobic and π-alkyl interactions with residues such as Ala145, Ile144, and Phe202, which are known to support ligand stability within the channel pore. This overall interaction pattern suggests that these compounds may serve as useful sodium channel blockers, even though slight variations were noted, such as carbon-hydrogen bonding with Phe198 rather than conventional hydrogen bonding—an observation supported by recent research demonstrating the importance of hydrophobic and aromatic interactions in anchoring ligands within sodium channel binding sites.

3.2. Pharmacokinetic and ADME Studies

Tables 5 and 6 summarize the compounds' pharmacokinetic properties, showing that most derivatives possess desirable drug-like features. According to Lipinski's Rule of Five, most compounds show good oral bioavailability potential (Table 5). Notably, ten compounds—Cp1, Cp3, Cp4, Cp8, Cp9, Cp10, Cp12, Cp13, Cp14, and Cp15—were predicted to penetrate the blood-brain barrier (BBB), an essential requirement for central nervous system activity. As further illustrated by the graphical representation of ADME features in Figure 6, these compounds occupy a physicochemical region suitable for CNS-active drugs, consistent with known determinants of BBB permeability such as molecular size, polarity, and lipophilicity [36–41].

2026, Vol. 3, Article ID. 2026.0020
https://doi.org/10.69709/MolModC.2026.199313

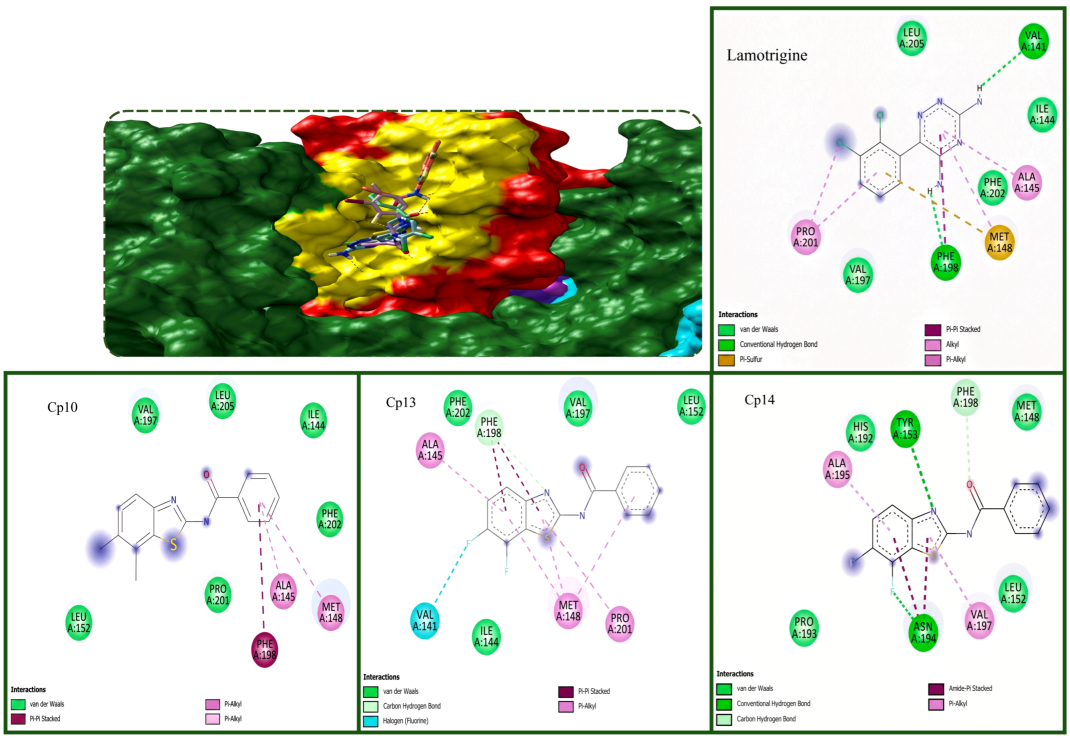


Figure 4: Comparison of molecular surface and 2D interaction patterns of lamotrigine and selected compounds (Cp10, Cp13, and Cp14) within the Nav*Ms* active site.

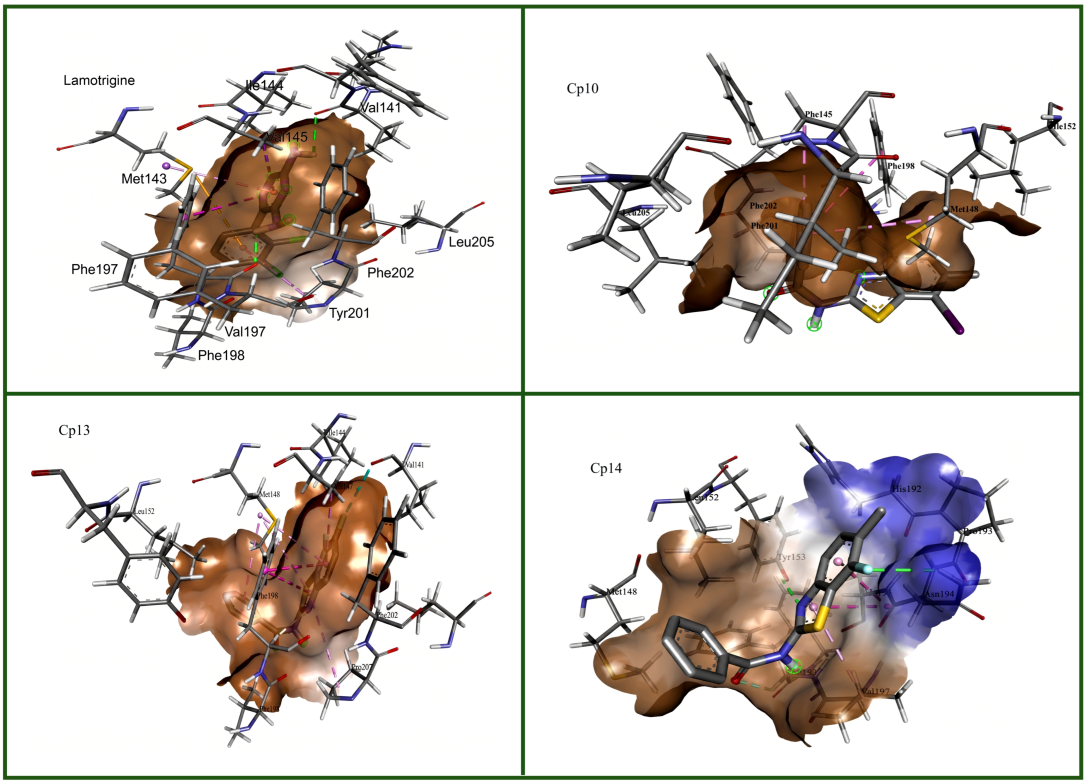


Figure 5: Structural depiction of 3D interactions between lamotrigine and selected compounds (Cp10, Cp13, and Cp14) at the Nav*Ms* active site.

Table 5: Lipinski's Rule-of-Five-based prediction of oral bioavailability.

Compounds No	Log P	Molecular Weight	H-Bond Donors	H-Bond Acceptors
Compound 1	3.05	288.75	1	2
Compound 2	2.85	333.75	1	4
Compound 3	3.16	323.20	1	2
Compound 4	3.28	300.35	1	3
Compound 5	1.03	344.30	1	6
Compound 6	1.46	314.36	1	4
Compound 7	1.89	314.36	1	7
Compound 8	2.77	286.32	1	3
Compound 9	3.40	414.65	1	2
Compound 10	3.54	394.23	1	2
Compound 11	2.96	410.23	1	3
Compound 12	3.13	394.23	1	2
Compound 13	3.32	290.29	1	4
Compound 14	3.17	286.32	1	3
Compound 15	3.57	323.20	1	2
Reference (Vigabatrin)	0.28	129.16	2	3
Reference (Lamotrigine)	1.75	256.09	2	3

Note: In accordance with Lipinski's Rule of Five, compounds should possess a molecular weight $\leq$ 500 Da, logP $\leq$ 5, no more than 5 hydrogen bond donors, and no more than 10 hydrogen bond acceptors.

Table 6: Predicted SwissADME parameters of the fifteen compounds compared with those of the reference drugs.

Compounds No.	GIA	BBB Permeant	P-gp
Cp1	High	1	None
Cp2	High	0	None
Cp3	High	1	None
Cp4	High	1	None
Cp5	Low	0	None
Cp6	High	0	None
Cp7	High	0	None
Cp8	High	1	None
Cp9	High	1	None
Cp10	High	1	None
Cp11	High	0	None
Cp12	High	1	None
Cp13	High	1	None
Cp14	High	1	None
Cp15	High	1	None
Reference (Vigabatrin)	High	0	None
Reference (Lamotrigine)	High	0	Enzyme inhibitor

GIA corresponds to gastrointestinal absorption, BBB describes predicted blood-brain barrier penetration (0 = absent, 1 = present), and P-gp denotes P-glycoprotein interaction status.

Furthermore, unlike lamotrigine—which is known to be influenced by P-gp-mediated transport—none of the compounds were predicted to interact significantly with P-glycoprotein (P-gp). Because P-glycoprotein is required for lamotrigine to cross the blood-brain barrier, this finding underscores the role this transporter plays in the inadequate CNS absorption of numerous antiepileptic drugs [42–44].

Additionally, the majority of compounds satisfied Lipinski's Rule of Five, indicating favorable drug-likeness and oral bioavailability [36–38]. Supported by graphical analyses, the resulting ADME profiles place the lead compounds within the optimal physicochemical space for CNS-active drugs, balancing lipophilicity, polarity, and molecular weight [36–41].

2026, Vol. 3, Article ID. 2026.0020
https://doi.org/10.69709/MolModC.2026.199313

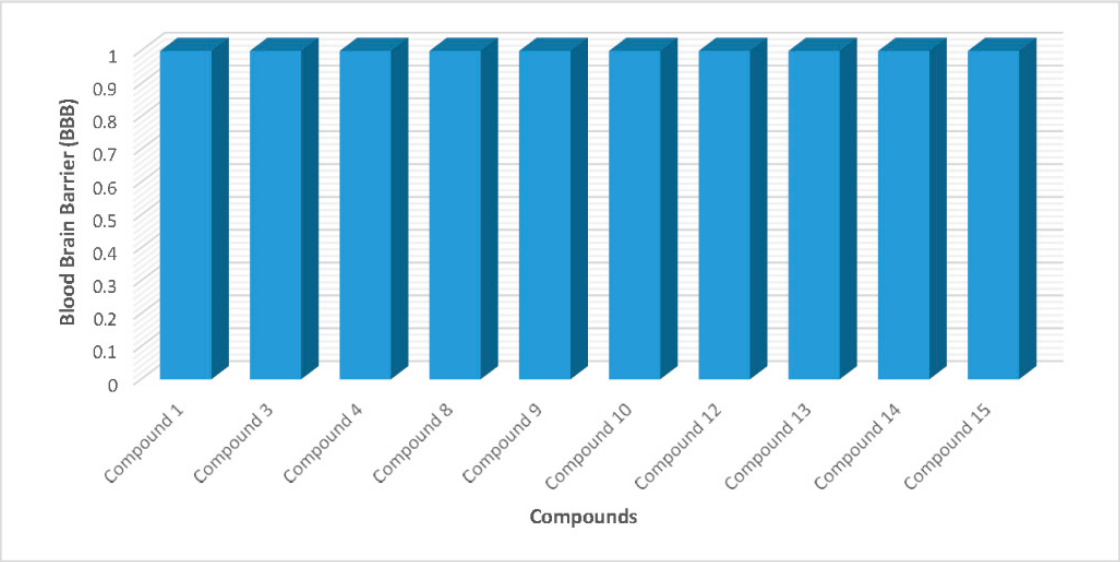


Figure 6: Graphical representation of compounds exhibiting blood-brain barrier permeability.

4. Conclusions

Based on the molecular docking results, several N-(substituted-1,3-benzothiazol-2-yl)benzamide derivatives demonstrated favorable interactions within the active sites of both target proteins. Seven compounds (Cp1, Cp3, Cp7, Cp10, Cp12, Cp13, and Cp14) exhibited promising binding affinity toward GABA-AT, while three compounds (Cp10, Cp13, and Cp14) also showed effective interactions with Nav*Ms*. These derivatives further displayed favorable ADME characteristics supportive of central nervous system delivery. Among them, Cp1, Cp3, Cp7, Cp10, Cp12, Cp13, and Cp14 were identified as the most promising lead candidates, exhibiting notable potential as anticonvulsant agents.

List of Abbreviations

ADME	Absorption Distribution Metabolism and Elimination
BBB	Blood Brain Barrier
CNS	Central Nervous System
Cp	Compound
GABA	Gamma Amino Butyric Acid
GABA-AT	Gamma-Aminobutyric Acid-Aminotransferase
GIA	Gastrointestinal Absorption
MDL	Molecular Design Limited
MMFF	Molecular Mechanics Force Fields
Nav*Ms*	Voltage-gated Sodium Channels Protein from *Magnetococcus marinus*
Navs	Voltage-gated Sodium Channels
PDB	Protein Data Bank
P-gp	P-glycoprotein
PK	Pharmacokinetic
RCSB	Research Collaboratory for Structural Bioinformatics
RMSD	Root Mean Square Deviation
SD	Structure Data
2D	Two-Dimensional
3D	Three-Dimensional

Author Contributions

Conceptualization, Software, Methodology, Investigation, and Validation: A.R.; Data curation: A.R., A.Y.I., A.M.M., H.S.H., A.H.N., M.G.M., R.B., M.S., and I.J.M.; Formal analysis: A.R., A.Y.I., A.M.M., H.S.H., A.H.N., M.G.M., R.B., M.S., and I.J.M.; Visualization: A.Y.I.; Supervision: A.Y.I., A.M.M., H.S.H., A.H.N., and M.G.M.; Writing—original draft: A.R.; Writing—review and editing: A.Y.I., A.M.M., H.S.H., A.H.N., M.G.M., R.B., M.S., and I.J.M. All authors have read and approved the published version of the manuscript.

Availability of Data and Materials

All data used in this study were generated through computational experiments and are included in this manuscript; further data can be obtained from the corresponding author upon request.

Conflicts of Interest

The authors declare no conflicts of interest.

Funding

The study did not receive any external funding and was conducted using only institutional resources.

Acknowledgments

The authors sincerely acknowledge the Department of Pharmaceutical and Medicinal Chemistry, Faculty of Pharmaceutical Sciences, Ahmadu Bello University, Zaria, Nigeria, for providing essential research facilities and support for this study. The authors also thank the Department of Pharmaceutical and Medicinal Chemistry, Gombe State University, Gombe, Nigeria, and the Department of Pharmaceutical and Medicinal Chemistry, Kaduna State University, Kaduna, Nigeria, for providing additional research facilities that contributed to the successful completion of this work.

AI Declaration

The authors acknowledge the use of Quillbot AI tool during the preparation of this manuscript solely for language enhancement, grammar correction, and readability improvement; this tool was not used for study concept or design, data collection, experimental computation, results interpretation, or formulation of scientific conclusions. All intellectual content, scientific interpretations, and conclusions presented in this manuscript remain the sole responsibility of the authors, who have critically reviewed, checked, and approved the final version of the manuscript and accept full responsibility for its accuracy, integrity, and originality.

References

[1] WHO. Intersectoral Global Action Plan on Epilepsy and Other Neurological Disorders 2022–2031. 2022. Available online: https://www.who.int/news/item/12-01-2022-draft-intersectoral-global-action-plan-on-epilepsy-and-other-neurological-disorders-2022-2031 (accessed on 6 April 2022).

[2] Fonseca-Barriendos, D.; Frías-Soria, C.L.; Pérez-Pérez, D.; Gómez-López, R.; Borroto-Escuela, D.O.; Rocha, L. Drug-Resistant Epilepsy: Drug Target Hypothesis and Beyond the Receptors. *Epilepsia Open* **2022**, *7*, S23–S33. [CrossRef] [PubMed]

[3] Benny, F.; Oh, J.M.; Kumar, S.; Abdelgawad, M.A.; Ghoneim, M.M.; Abdel-Bakky, M.S.; Kukerti, N.; Jose, J.; Kim, H.; Mathew, B. Isatin-Based Benzyloxybenzene Derivatives as Monoamine Oxidase Inhibitors with Neuroprotective Effect Targeting Neurodegenerative Disease Treatment. *RSC Adv.* **2023**, *13*, 35240–35250. [CrossRef] [PubMed]

[4] Savoca, G.; Gianfredi, A.; Bartolini, L. The Development of Epilepsy Following CNS Viral Infections: Mechanisms. *Curr. Neurol. Neurosci. Rep.* **2025**, *25*, 2. [CrossRef] [PubMed]

[5] Matsuyama, T.; Horinouchi, T.; Nakamura, Y.; Ishikawa, S.; Hashimoto, N.; Kusumi, I. Tolerability of Perampanel: A Retrospective Study at the Department of Psychiatry. *Epilepsy Behav.* **2024**, *156*, 109797. [CrossRef] [PubMed]

[6] Belete, T.M. Recent Progress in the Development of New Antiepileptic Drugs with Novel Targets. *Ann. Neurosci.* **2023**, *30*, 262–276. [CrossRef] [PubMed]

[7] Valipour, M.; Ghasemian, M.; Karima, S.; Zakeri Khatir, Z.; Aghamiri, H.; Shaki, F.; Akbari, S.; Talebpour Amiri, F.; Hosseini, A.; Jafari-Sabet, M.; et al. Design, Synthesis, and Structure-Activity Relationships of Five-Membered Heterocyclic Incorporated Aryl(alkyl)azoles: From Antiproliferative Thiazoles to Safer Anticonvulsant Oxadiazoles. *Bioorg. Chem.* **2025**, *155*, 108117. [CrossRef] [PubMed]

[8] Grover, G.; Pal, R.; Bhatia, R.; Yar, M.S.; Nath, R.; Singh, S.; Raj, K.; Kumar, B.; Akhtar, M.J. Design, Synthesis and Pharmacological Evaluation of Aryl Oxadiazole Linked 1,2,4-Triazine Derivatives as Anticonvulsant Agents. *Med. Chem. Res.* **2022**, *31*, 781–793. [View Online]

[9] Alhamzani, A.G.; Yousef, T.A.; Abou-Krisha, M.M.; Raghu, M.S.; Kumar, K.Y.;; Prashanth, M.K.; Jeon, B.-H. Design, Synthesis, Molecular Docking and Pharmacological Evaluation of Novel Triazine-Based Triazole Derivatives as Potential Anticonvulsant Agents. *Bioorg. Med. Chem. Lett.* **2022**, *77*, 129042. [CrossRef] [PubMed]

[10] Abd-Allah, W.H.; Abd El-Maksoud, M.S.; Elbaset, M.A.; Hessin, A.F.; Hassan, R.M. Design and Synthesis of Novel Cycloalkanecarboxamide Parabanic Acid Hybrids as Anticonvulsants. *Med. Chem. Res.* **2024**, *33*, 89–106. [CrossRef]

[11] Kumar, G.; Singh, S.; Negi, M.; Abhishek, S. An In-Depth Analysis of Benzothiazole Derivatives: Structure, Properties, and Applications. *Int. J. Sci. Res. Sci. Technol.* **2024**, *11*, 17–42. [CrossRef]

[12] Wang, Q.; Nilsson, T.; Eriksson, L.; Szabó, K.J. Sulfenofunctionalization of Chiral α-Trifluoromethyl Allylboronic Acids: Asymmetric Synthesis of SCF3, SCF2 R, SCN and SAr Compounds. *Angew. Chem. Int. Ed.* **2022**, *61*, e202210509. [CrossRef] [PubMed]

[13] Salaria, P.; Akshinthala, P.; Kapavarapu, R.; Reddy, A.M. Identification of Novel C-15 Fluoro Isosteviol Derivatives for GABA-AT Inhibition by *In Silico* Investigations. *J. Mol. Model.* **2023**, *29*, 76. [CrossRef] [PubMed]

[14] Bai, F.; Song, Y.; Cao, Y.; Ban, M.; Zhang, Z.; Sun, Y.; Feng, Y.; Li, C. Scorpion Neurotoxin Syb-prII-1 Exerts Analgesic Effect Through Nav1.8 Channel and MAPKs Pathway. *Int. J. Mol. Sci.* **2022**, *23*, 7065. [CrossRef] [PubMed]

[15] Kanemura, H. Therapeutic Strategies in Children with Epilepsy: A Quality-of-Life-Related Perspective. *J. Clin. Med.* **2024**, *13*, 405. [CrossRef] [PubMed]

[16] Hasan, M.R.; Alsaiari, A.A.; Fakhurji, B.Z.; Molla, M.H.R.; Asseri, A.H.; Sumon, M.A.A.; Park, M.N.;

Ahammad, F.; Kim, B. Application of Mathematical Modeling and Computational Tools in the Modern Drug Design and Development Process. *Molecules* **2022**, *27*, 4169. [CrossRef] [PubMed]

[17] Vanshita; Garg, A.; Dewangan, H.K. Recent Advances in Drug Design and Delivery Across Biological Barriers Using Computational Models. *Lett. Drug Des. Discov.* **2022**, *19*, 865–876. [CrossRef]

[18] Niu, Y.; Lin, P. Advances of Computer-Aided Drug Design (CADD) in the Development of Anti-Alzheimer's-Disease Drugs. *Drug Discov. Today* **2023**, *28*, 103665. [CrossRef] [PubMed]

[19] Rufa'i, A.; Idris, A.Y.; Musa, A.M.; Hassan, H.S.; Nasiru, A.H.; Magaji, M.G. Molecular Docking and *In Silico* Pharmacokinetic Analysis of 1,3-Benzothiazole-2-amine Derivatives as Anticonvulsants. *J. Taibah Univ. Med. Sci.* **2025**, *20*, 629–642. [CrossRef] [PubMed]

[20] Trott, O.; Olson, A.J. AutoDock Vina: Improving the Speed and Accuracy of Docking with a New Scoring Function, Efficient Optimization, and Multithreading. *J. Comput. Chem.* **2010**, *31*, 455–461. [CrossRef] [PubMed]

[21] Eldeeb, M.; Sanad, E.F.; Ragab, A.; Ammar, Y.A.; Mahmoud, K.; Ali, M.M.; Hamdy, N.M. Anticancer Effects with Molecular Docking Confirmation of Newly Synthesized Isatin Sulfonamide Molecular Hybrid Derivatives Against Hepatic Cancer Cell Lines. *Biomedicines* **2022**, *10*, 722. [CrossRef] [PubMed]

[22] Bansod, G.; Singh, A.V.; Bhardwaj, P.; Rai, T.; Nakhale, S.V.; Shelar, A.; Patil, R.; Laux, P.; Luch, A.; Osgood, C.J.; et al. Decoding Tattoo and Permanent Makeup Pigments: Linking Physicochemical Properties to Absorption, Distribution, Metabolism, and Elimination Profiles Using Quantitative Structure–Activity Relationship (QSAR)-Based New Approach Methodologies (NAMs). *Adv. Intell. Discov.* **2026**, *2*, e202500027. [CrossRef]

[23] Marzouk, A.A.; Bass, A.K.A.; Ahmed, M.S.; Abdelhamid, A.A.; Elshaier, Y.A.M.M.; Salman, A.M.M.; Aly, O.M. Design, Synthesis and Anticonvulsant Activity of New Imidazolidindione and Imidazole Derivatives. *Bioorg. Chem.* **2020**, *101*, 104020. [CrossRef] [PubMed]

[24] Pantaleão, S.Q.; Fernandes, P.O.; Gonçalves, J.E.; Maltarollo, V.G.; Honorio, K.M. Recent Advances in the Prediction of Pharmacokinetics Properties in Drug Design Studies: A Review. *ChemMedChem* **2022**, *17*, e202100542. [CrossRef] [PubMed]

[25] Lipinski, C.A.; Lombardo, F.; Dominy, B.W.; Feeney, P.J. Experimental and Computational Approaches to Estimate Solubility and Permeability in Drug Discovery and Development Settings. *Adv. Drug Deliv. Rev.* **2012**, *64*, 4–17. [CrossRef]

[26] Das, S.K.; Mahapatra, A.; Sanket, S. Phytochemical Characterization and Bioactivity Assessment of *Avicennia officinalis* L. Bark Extracts. *Anal. Chem. Lett.* **2024**, *14*, 369–381. [CrossRef]

[27] Mendake, R.A.; Hatwar, P.R.; Bakal, R.L.; Hiwe, K.A.; Barewar, S.S. Advance and opportunities in Nanoparticle Drug Delivery for Central Nervous System Disorders: A Review of Current Advances. *GSC Biol. Pharm. Sci.* **2024**, *27*, 044–058. [CrossRef]

[28] Matošević, A.; Opsenica, D.M.; Bartolić, M.; Maraković, N.; Stoilković, A.; Komatović, K.; Zandona, A.; Žunec, S.; Bosak, A. Derivatives of Amodiaquine as Potent Human Cholinesterases Inhibitors: Implication for Treatment of Alzheimer's Disease. *Molecules* **2024**, *29*, 5357. [CrossRef] [PubMed]

[29] Chivukula, N.; Madgaonkar, S.R.; Marigoudar, S.R.; Sharma, K.V.; Kishore, V.; Singh, A.V.; Samal, A. TICToK: A Comprehensive Knowledgebase of Tattoo Ink Chemicals and Investigation of Their Associated Toxicities and Regulations. *bioRxiv* **2025**. [CrossRef]

[30] Aboutabl, M.E.; Hassan, R.M.; El-Azzouny, A.A.; Aboul-Enein, M.N.; Abd-Allah, W.H. Design and Synthesis of Novel Parabanic Acid Derivatives as Anticonvulsants. *Bioorg. Chem.* **2020**, *94*, 103473. [CrossRef] [PubMed]

[31] Abd-Allah, W.H.; Osman, E.E.A.; Anwar, M.A.E.M.; Attia, H.N.; El Moghazy, S.M. Design, Synthesis and Docking Studies of Novel Benzopyrone Derivatives as Anticonvulsants. *Bioorg. Chem.* **2020**, *98*, 103738. [CrossRef] [PubMed]

[32] Choudhary, S.; Dubey, A.; Singh, A.; Zamboni, P.; Gupta, N.; Singh, R.; Tisato, V.; Aggarwal, L.M.; Gemmati, D. Engineering the Microenvironment: Advanced Biomaterials for Humanized In Vitro Immunotoxicology and Carcinogenicity Assessment. *Explor. BioMat-X* **2025**, *2*, 101351. [CrossRef]

[33] Bagnéris, C.; DeCaen, P.G.; Naylor, C.E.; Pryde, D.C.; Nobeli, I.; Clapham, D.E.; Wallace, B.A. Prokaryotic Nav*Ms* Channel as a Structural and Functional Model for Eukaryotic Sodium Channel Antagonism. *Proc. Natl. Acad. Sci. U.S.A.* **2014**, *111*, 8428–8433. [CrossRef] [PubMed]

[34] Sait, L.G.; Sula, A.; Ghovanloo, M.-R.; Hollingworth, D.; Ruben, P.C.; Wallace, B.A. Cannabidiol Interactions with Voltage-Gated Sodium Channels. *eLife* **2020**, *9*, e58593. [CrossRef] [PubMed]

[35] McCollum, M.M.; Larmore, M.; Ishihara, S.; Ng, L.C.T.; Kimura, L.F.; Guadarrama, E.; Ta, M.C.; Vien, T.N.; Frost, G.B.; Scheidt, K.A.; et al. Targeting the Tamoxifen Receptor Within Sodium Channels to Block Osteoarthritic Pain. *Cell Rep.* **2022**, *40*, 111248. [CrossRef] [PubMed]

[36] Pajouhesh, H.; Lenz, G.R. Medicinal Chemical Properties of Successful Central Nervous System Drugs. *NeuroRx* **2005**, *2*, 541–553. [CrossRef] [PubMed]

[37] Bisht, N.; Singh, B.K. Structure Based Virtual Screening, Molecular Docking Studies and Modification of Hydantoin Nucleus Analogues as Anticonvulsants. *Indian J. Chem.* **2018**, *57B*, 1514–1525. [View Online]

[38] Verma, S.D.; Passerat de la Chapelle, E.; Malkani, S.; Juran, C.M.; Boyko, V.; Costes, S.V.; Cekanaviciute, E. Astrocytes Regulate Vascular Endothelial

Responses to Simulated Deep Space Radiation in a Human Organ-on-a-Chip Model. *Front. Immunol.* **2022**, *13*, 864923. [CrossRef] [PubMed]

[39] Chi, G.F.; Khan, S.; Başar, Y.; Kuete, J.R.N.; Matieta, V.Y.; Kuete, J.B.T.; Megaptche, J.F.; Chongong, M.A.; Yenigün, S.; Ayimele, G.A.; et al. Antibacterial Flavonoids from *Tetrapleura tetraptera* (Fabaceae) Fruit Pulp, *In Silico* Studies. *S. Afr. J. Bot.* **2025**, *180*, 96–106. [CrossRef]

[40] Başar, Y.; Yenigün, S.; Kocaman, A.Y.; Chi, G.F.; Ozturk, E.; Demirtaş, İ.; Tel, A.Z. Cytotoxicity of *Dysphania botrys* L. Extracts Against HEPG2 and SAOS-2, *In Vitro* and *In Silico*. *Chem. Biodivers.* **2025**, *22*, e01615. [CrossRef] [PubMed]

[41] Başar, Y.; Yigit, A.; Chi, G.F.; Sunyar, B.; Demirtaş, İ. Green Synthesised Silver Nanoparticle From *Cotoneaster horizontalis*, *In Vitro* and *In Silico* Antibacterial Properties. *Chem. Biodivers.* **2026**, *23*, e02265. [CrossRef] [PubMed]

[42] Li, J.; Zhang, Z.; Zhang, B.; Yan, X.; Fan, K. Transferrin Receptor 1 Targeted Nanomedicine for Brain Tumor Therapy. *Biomater. Sci.* **2023**, *11*, 3394–3413. [CrossRef] [PubMed]

[43] Ping, H.; Ding, D.; Zhu, G.; Wang, J.; Zhang, J. Advancements in the Application of Nanotechnology for the Management of Epileptic Seizures. *Acta Epileptol.* **2024**, *6*, 23. [CrossRef] [PubMed]

[44] Villa, M.; Wu, J.; Hansen, S.; Pahnke, J. Emerging Role of ABC Transporters in Glia Cells in Health and Diseases of the Central Nervous System. *Cells* **2024**, *13*, 740. [CrossRef] [PubMed]

Disclaimer/Publisher's Note: The views expressed in this article are those of the author(s) and do not necessarily reflect the views of the publisher or editors. The publisher and editors assume no responsibility for any injury or damage resulting from the use of information contained herein.